

NASA Technical Memorandum 4550

Launch-Pad Abort Capabilities of the HL-20 Lifting Body

*E. Bruce Jackson and Robert A. Rivers
Langley Research Center • Hampton, Virginia*

*Rajiv S. Chowdhry
Lockheed Engineering & Sciences Company • Hampton, Virginia*

*W. A. Ragsdale and David W. Geyer
Unisys Corporation • Hampton, Virginia*

National Aeronautics and Space Administration
Langley Research Center • Hampton, Virginia 23681-0001

May 1994



Abstract

The capability of the HL-20 lifting body to perform an abort maneuver from the launch pad to a horizontal landing was studied. The study involved both piloted and batch simulation models of the vehicle. A point-mass model of the vehicle was used for trajectory optimization studies. The piloted simulation was performed in the Langley Visual/Motion Simulator in the fixed-base mode. A candidate maneuver was developed and refined for the worst-case launch-pad-to-landing-site geometry with an iterative procedure of off-line maneuver analysis followed by piloted evaluations and heuristic improvements to the candidate maneuver. The resulting maneuver demonstrates the launch-site abort capability of the HL-20 and dictates requirements for nominal abort-motor performance. The sensitivity of the maneuver to variations in several design parameters was documented.

Introduction

The HL-20 has been proposed as a crew transport vehicle for the personnel launch system. The current baseline design is a 20 000-lb lifting body with a maximum subsonic lift-drag ratio of 4.3 that is capable of being launched vertically into low Earth orbit by an expendable launch vehicle and can be landed horizontally following reentry. Figure 1 is a three-view drawing of the concept. The vehicle is designed to carry a crew of two and up to eight passengers to and from low Earth orbit. Both manual and automatic landing capabilities are planned (ref. 1).

A 6700-lb adapter module will be used to connect the HL-20 to the launch vehicle. (See fig. 2.) This adapter design will include a launch escape system that is intended to thrust the HL-20 away from the booster in case of a malfunction either during the actual launch or on the pad prior to launch (on-pad abort). Acceleration levels on the order of $8g$'s ($1g = 32.2 \text{ ft/sec}^2$) would be required to propel the vehicle a safe distance away from a malfunctioning booster. After a specified time, the abort-motor thrust would drop to approximately $1g$ for an additional specified amount of time to avoid excessive velocities and associated drag. The adapter module would be jettisoned following abort-motor burnout.

The lift-drag ratio of the initial HL-20 configuration precluded a glide to a nearby runway. Thus, the original on-pad abort scenarios were similar to those for previous manned capsules, that is, an abort to ocean landing with a recovery parachute (ref. 2). Additional aerodynamic refinements of the HL-20 configuration led to increased subsonic lift-drag ratios, and a higher performance abort motor was specified for the launch escape system (ref. 3). These improvements raised the possibility of performing a conven-

tional horizontal landing following an on-pad abort (pad abort to runway).

A previous manned space project, the X-20 Dyna-Soar, was designed to have a pad abort-to-runway capability. To verify the feasibility of this abort contingency, an in-flight simulation study was conducted in a delta-wing interceptor aircraft (ref. 4). The trajectory flown in the aircraft consisted of a low-level, high-speed entry into a vertical pull-up at a predetermined location to simulate abort initiation. This maneuver was followed by a pullover to the horizon, a roll maneuver to an upright wings-level attitude, and a 180° turn to landing. The relationship between the pad and the skid strip in the X-20 launch scenario was different than that proposed for the HL-20.

A study was initiated to determine whether the HL-20 vehicle could successfully be maneuvered to a runway landing in the event of an on-pad abort and to determine what design parameters would improve the feasibility of such a maneuver. The results of the study are presented herein.

Symbols and Abbreviations

KEAS	knots equivalent airspeed
L/D	lift-drag ratio
OMS	orbital maneuvering subsystem
SRM	solid rocket motor
V	velocity, ft/sec
α	angle of attack, deg
θ	pitch angle, deg
ϕ	bank angle, deg

Simulation Models

To evaluate the pad-abort-to-runway scenario, a candidate maneuver was developed and analyzed with off-line and real-time simulation tools. The real-time piloted simulation was used to explore possible abort maneuvers; the off-line simulation was used to arrive at a numerically optimal trajectory. The piloted simulation was then used to validate the optimal trajectory and to suggest simplifications to the maneuver that would make it easier to perform. The piloted simulation tests were performed in a generic transport-type cockpit (fig. 3) with a left-hand side stick, a hydraulic control loader, forward and left-side out-the-window displays, head-down instrumentation and displays, and a simulated wide-field-of-view head-up display. The motion cueing system was not employed for these tests because of motion performance limitations.

The math model used in the piloted simulation was derived from an existing HL-20 approach-and-landing simulation model (refs. 5 and 6). Modifications included adding a model of the steerable abort motor with thrust and pitch-roll torques specified as a function of time, modeling the orbital maneuvering subsystem (OMS) rocket motors, and increasing the vehicle mass properties appropriately. Modifications to the flight-director and autopilot control laws, the control-law mode-switching logic, and simulation initialization logic were required. Head-up and head-down flight displays were modified to assist in pilot orientation during the maneuver.

The off-line simulation employed a point-mass model that used optimal trajectory simulation software (ref. 7). The simplified aerodynamics of this model consisted of lift and drag coefficients as a function of Mach number and angle of attack. Control deflection, landing gear, and ground effects were not modeled. Some performance differences between the off-line and piloted simulations are apparent; however, the optimal maneuvers developed with the off-line simulation provided insight into a practical and efficient abort maneuver for manual or automatic flight control.

Abort Trajectory Design

A set of probable launch-pad/runway geometries, vehicle orientations, and abort maneuvers was initially considered. The set included simulated aborts from Kennedy Space Center launch pads 39A, 40, and 41 with simulated landings at both the Shuttle Landing Facility and the Cape Canaveral Air Force Station skid strip. The orientations of the launch pads and landing facilities are shown in figure 4. Candidate abort scenarios included various orientations

of the launch stack in which the vertical fin of the HL-20 was pointed due east, slightly south of east, slightly north of west, or in an optimal direction. Some of these vehicle orientations were dictated by launch-pad constraints.

Nominal touchdown speed for the abort cases was increased from 200 knots equivalent airspeed (KEAS), the nominal end-of-mission value to 230 KEAS as a result of the heavier weight of the vehicle with all consumables still aboard (25 800 lb versus 19 100 lb). This difference mandated a higher minimum speed at the beginning of the preflare maneuver (275 KEAS versus 250 KEAS).

Trial Trajectory

As a starting point in this investigation, an optimized trajectory was generated for one of the abort situations (pad 40 to skid-strip runway 13) using angle of attack and bank angle as the control variables. The starting point for the maneuver was 100 ft above launch pad 40 with an initial velocity of 50 ft/sec (to avoid numerical problems). Final conditions were specified to be a trimmed glide at 450 ft/sec (266 knots) over the approach end of runway 13 and aligned with the runway heading. Bank angle was constrained to $\pm 30^\circ$ and roll rate to $\pm 28.6^\circ/\text{sec}$ (± 0.5 rad/sec). Angle of attack was constrained to 0° to 30° , and angle-of-attack rate was constrained to $\pm 5.7^\circ/\text{sec}$ (± 0.1 rad/sec). The optimization program was free to pick an initial flight-path angle and heading, as well as angle of attack and bank-angle control trajectories. A 3-sec, $8g$ abort-motor thrust pulse at the start of the maneuver, followed by a constant 1500-lb thrust from the simulated OMS engines, was modeled as the only energy addition to the problem. The optimizer was asked to maximize the altitude over the runway threshold (threshold crossing height).

The resulting optimal trajectory (fig. 5) indicated an initial flight-path angle of approximately 45° was preferred; this angle corresponds with the launch angle of ballistic projectiles to achieve theoretical maximum range in a vacuum. The optimal turn to final approach was a gradual roll to intercept the final-approach course at approximately the same time the roll-angle limit was reached. The altitude predicted over the runway threshold was 1193 ft. This trial trajectory showed the benefit of steerable abort motors that would allow rapid modification of the vehicle orientation at the beginning of the maneuver to obtain optimal heading and flight-path angles as soon as possible. It also indicated that an optimal trajectory would be difficult for a pilot to follow, because of the continuous variation in flight

conditions, and that the inevitable deviation from the preplanned trajectory would require recomputation of a new optimal trajectory from the new vehicle state.

Other Candidate Trajectories

In addition to the abort to runway 13 for pad 40, a candidate trajectory for each of the other situations was developed in the piloted simulation. Early-abort maneuver candidates included a pullover followed by a half-roll (for head-down aborts), pushover (for head-up aborts), and a modified "sliceback" or wingover maneuver for abort orientations that require a heading change. (In this context, the term head-up or head-down refers to the attitude of the crew during the initial portion of the abort.) The improvement in maneuver performance gained by immediately rolling and pitching the vehicle to an optimal heading and attitude led to the adoption of steerable abort motors. Abortions both with and without firing the OMS and with modified abort-motor thrust profiles were studied.

Worst-Case Trajectory

From these preliminary investigations, the worst-case launch-pad-to-runway geometry was selected for further study. This worst-case geometry involved an abort from the southernmost Shuttle launch pad, pad 39A, to the skid-strip runway 13, a straight-line distance of 8.3 n.mi., compared with 5.3 n.mi. for the trial trajectory. This worst-case scenario assumed a primary abort-motor duration of 3.5 sec, a set of sustainer motors that provided 33 000 lb thrust for 11.5 sec, and no OMS thrust, compared with a 3-sec primary abort-motor thrust duration, no sustainer motor thrust, and a constant 1500 lb thrust provided by the OMS engines throughout the trial trajectory. The primary abort-motor thrust was constant at 248 800 lb in both cases. The vertical fin of the HL-20 on the launch pad was assumed to be pointed 100° (clockwise from true north). This alignment would correspond to an eastward head-down launch configuration and would require an immediate right roll to orient the vehicle for a head-up abort. Winds were assumed to be steady at 22 knots and were assumed to be coming directly from the runway to the launch pad.

The focus of the research then shifted to the development of a simplified abort maneuver that was as efficient as possible but that could be flown repeatedly by a pilot. It is anticipated that, given the suddenness of the abort maneuver and the rapid rotation of the vehicle, automatic control of the vehicle is required for at least the initial part of

the maneuver; however, the simplified maneuver was developed with a pilot and was demonstrated by both the pilot and an automatic flight-control system. This automatic flight-control system allowed manual takeover at any point.

Initial steering. The worst-case abort maneuver from pad 39A was begun with a 3.5-sec, 248 800-lb burn of the abort motors. The abort motors were assumed to be steerable and were used to rapidly roll the vehicle to a 182° heading to begin a head-up maneuver to the runway. The motors then pitched the vehicle down to a 45° pitch attitude. These maneuvers were completed in approximately the first second of the abort. Figure 6 shows the abort-motor thrust and torque time histories used in the simulation. After 3.5 sec, the abort-motor thrust was decreased to 33 000 lb; this reduction provided a sustainer thrust level of nearly 1g for the next 11.5 sec. (This value for the duration of the sustainer motor burn was determined after several trials.) The pilot was asked to hold a 45° flight-path angle by using the head-up-display (HUD) pitch ladder and velocity vector (fig. 7) until abort-motor burnout, at which time the adapter module was jettisoned.

Pushover maneuver. Following abort-motor burnout, a zero-alpha pushover maneuver was executed. The pilot performed this maneuver by moving the boresight marker to coincide with the velocity vector on the HUD. Nominal apogee conditions were 10 633 ft at 228 KEAS and at a distance of 13 240 ft downrange from the launch pad at 28 sec after initiation of the abort. The zero-alpha flight condition was maintained until a specified negative flight-path angle was reached.

Pullout maneuver. A pullout maneuver was then performed to achieve the nominal glide condition (300 KEAS at -14° flight-path angle), which was maintained until beginning the turn to final approach. The details of the maneuver were developed heuristically in the piloted simulation and consisted of following the zero-alpha flight condition until a flight-path condition of approximately -28° was reached at approximately 240 KEAS. Angle of attack was then increased over the next 25 sec to simultaneously achieve the nominal glide speed (300 KEAS) and flight-path angle (-14°); these conditions were maintained until starting the final turn maneuver. The rate at which the velocity vector was raised was limited by the requirement not to exceed the maximum lift-drag angle of attack (13°). Angles of attack above 13° resulted in rapid energy dissipation. This portion of the maneuver seemed to require

practice on the part of the pilot; a guidance algorithm would have been of some benefit but was not utilized.

Steady glide. To determine the best glide conditions, a set of trim cases was generated using the full nonlinear model for steady straight-ahead glide conditions at constant equivalent airspeed for various levels of OMS thrust. These trim curves are shown in figure 8. The nominal glide speed used in the simulation for the zero OMS thrust worst-case situation (300 KEAS and -14° flight path) was slightly faster than the best glide speed for the vehicle (265 KEAS) at the heavy-abort weight of 25 800 lb. This higher speed was chosen to improve penetration into the headwind and to match the entry speed of the final-turn maneuver.

Final-turn maneuver. The initial optimal point-mass solution (fig. 5) included a constantly varying bank angle in the turn to final. This maneuver was difficult for the pilot to perform consistently, and a nonoptimal, constant-bank-angle turn was more acceptable. A set of steep gliding turn trim cases was generated off-line for the full nonlinear vehicle model. This analysis generated a set of curves that showed that a bank angle of 49° could be sustained at 300 KEAS and with a load factor of 1.4. (See fig. 9.) During the 8000-ft-radius turn, the HL-20 lost approximately 65 ft of altitude per degree of heading change and maintained sufficient speed to complete the flare and landing maneuver. Turns performed at slower speeds could yield a slight improvement in turn efficiency (a 42° bank turn at 250 knots, for example, loses only 50 ft per deg), but insufficient altitude remains after the turn to accelerate for the landing flare and landing maneuver. Thus, the model with the 300-knot airspeed, 49° bank angle, and 8000-ft-radius turn was chosen for the final-turn maneuver.

Following the turn to final approach, an immediate flare and landing maneuver followed. Touchdown occurred at a nominal distance of 1931 ft down the runway.

Worst-case maneuver comparisons. A typical heuristic abort trajectory is shown in figure 10. This condition includes 22 knots of wind from 181° (clockwise from true north) and the abort-motor performance history shown in figure 4. This trajectory was flown manually following the method described previously. The threshold crossing height was 25.3 ft.

A fully automatic abort trajectory is shown in figure 11 for the same conditions as the manual trajectory. This control strategy employed the same

heuristic rules as the manual strategy, with the exception of holding a constant angle of attack from apogee to extended glide-slope intercept, which accounts for the differences in steady glide trajectory. Threshold crossing height is nearly the same as the manual case (24.8 ft).

Following the development of the heuristic trajectory in the piloted simulation, an optimal trajectory for the worst-case geometry was generated for comparison. The optimal trajectory is plotted in figure 12 and is replotted with the manual and automatic abort trajectories in figure 13. It is apparent that the optimal trajectory outperforms the heuristic trajectory, as would be expected. However, the optimal trajectory is generated with a simplified math model of the aircraft without control-surface deflection or pitch dynamics; therefore, there is a somewhat more optimistic prediction of vehicle performance. Also, the goal of the optimization algorithm was to achieve the highest possible threshold crossing height, subject to the constraints described previously. Threshold crossing height for the optimal trajectory is 3794 ft. This is an optimistic outcome, however, because of the simplified vehicle model.

Estimated Parametric Sensitivities

Modifications to the launch escape system and vehicle design parameters were explored to determine the sensitivity of the abort maneuver to changes in design parameters. Parametric variations in vehicle weight, steady winds, maximum lift-drag ratio, abort-motor thrust levels, and the effect of firing the OMS thrusters were studied and benefits were calculated. Threshold crossing height was estimated from the energy state of the vehicle at the beginning of the turn to final approach. This estimation was used to counter the large dispersion in landing conditions introduced by the difficult turn to final approach. This estimation method also allowed the use of several simulation runs that were made without any computer-generated imagery. Five runs were performed manually for each perturbation amount studied. Numerical results of the parametric study are given in table 1.

As shown in the table, the estimation method indicates that successful landings were possible, and indeed were accomplished, in all five trials of the baseline configuration (same as the worst-case scenario in the previous section, but without any winds); however, the headwind cases (the last two entries) indicate a small negative estimated threshold crossing height. During the actual runs with the 22-knot headwind, however, five successful landings (out of five attempts) were accomplished by landing slower

than the 230-knot target speed used in the estimation method. The 22-knot case clearly represented an absolute worst-case abort condition.

Concluding Remarks

As a result of this study, it was concluded that a successful launch pad-abort-to-runway landing could be performed both manually and automatically for worst-case conditions. A candidate abort maneuver was developed through analysis and pilot experimentation, and sensitivity of the maneuver to design parameter variation was determined. A guidance and control law to automatically perform the abort was developed that was successful in providing a safe landing in the case of crew incapacitation. Comparisons of the candidate maneuver with an optimal maneuver indicated that additional performance gains might be realized with additional refinement of the maneuver.

NASA Langley Research Center
Hampton, VA 23681-0001
March 2, 1994

References

1. Piland, William M.; Talay, Theodore A.; and Stone, Howard W.: Personnel Launch System Definition. IAF-90-160, Oct. 1990.
2. Naftel, J. Chris; Powell, Richard W.; and Talay, Theodore A.: Performance Assessment of a Space Station Rescue and Personnel/Logistics Vehicle. *J. Spacecr. & Rockets*, vol. 27, no. 1, Jan. Feb. 1990, pp. 76-81.
3. Naftel, J. C.; and Talay, T. A.: Ascent Abort Capability for the HL-20. *J. Spacecr. & Rockets*, vol. 30, no. 5, Sept. Oct. 1993, pp. 628-634.
4. Matranga, Gene J.; Dana, William H.; and Armstrong, Neil A.: *Flight-Simulated Off-the-Pad Escape and Landing Maneuvers for a Vertically Launched Hypersonic Glider*. NASA TM X-637, 1962.
5. Jackson, E. B.; Powell, Richard W.; and Ragsdale, W. A.: Utilization of Simulation Tools in the HL-20 Conceptual Design Process - Passenger-Carrying Lifting Body Portion of Personnel Launch System. *Technical Report AIAA Flight Simulation Technologies Conference*, 1991, pp. 358-367. (Available as AIAA-91-2955.)
6. Jackson, E. Bruce; Cruz, Christopher I.; Ragsdale, W. A.: *Real-Time Simulation Model of the HL-20 Lifting Body*. NASA TM-107580, 1992.
7. Paris, S. W.; Hargraves, C. R.; Nance, M. L.; Renz, R. S.; and Lajoie, R. M.: *Optimal Trajectories by Implicit Simulation. Volume II User's Manual*. AFWAL-TR-88-3057. Volume II, U.S. Air Force, Nov. 1988. (Available from DTIC as AD B134 377.)

Table 1. Estimated Parametric Sensitivities for Launch-Pad 39A Abort to Runway 13

[Averaged for 5 manual aborts; Baseline--3.5-sec abort motor,
11.5-sec sustainer motor, thrust-vector control, calm winds]

Varied parameter	Variation	Estimated threshold crossing height, ft	Threshold crossing-height difference, ft	Threshold crossing-height sensitivity
Baseline	--	104		
Sustainer duration	-1.5 sec	-1035	-1139	759 ft/sec
	+1.5 sec	1321	1217	811 ft/sec
Vehicle weight	+3000 lb	-2451	-2555	-0.85 ft/lb
	3000 lb	2799	2696	-0.90 ft/lb
Lift-drag ratio	-0.5	-1340	-1444	289 ft/0.1 L/D^a
	+0.5	1787	1684	337 ft/0.1 L/D
Abort motor duration	+0.2 sec	1415	1311	656 ft/0.1 sec
Abort motor thrust	-15 000 lb	-1283	-1386	92.4 ft/1000 lb
	+15 000 lb	1411	1307	87.1 ft/1000 lb
OMS thrust	+1000 lb	2027	1923	1.9 ft/lb
Headwind from 181°	+11 knots	-141	-245	22.3 ft/knot
	+22 knots	-207	-311	14.1 ft/knot

^aChange in baseline L/D by 0.1.

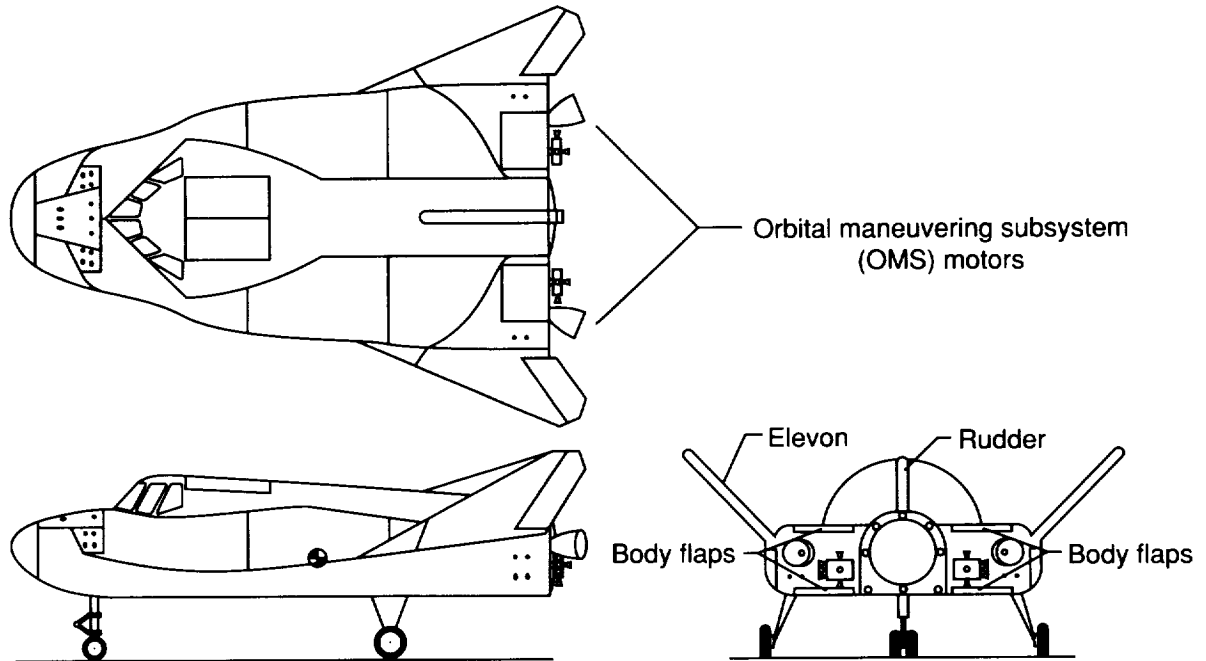


Figure 1. HL-20 lifting body.

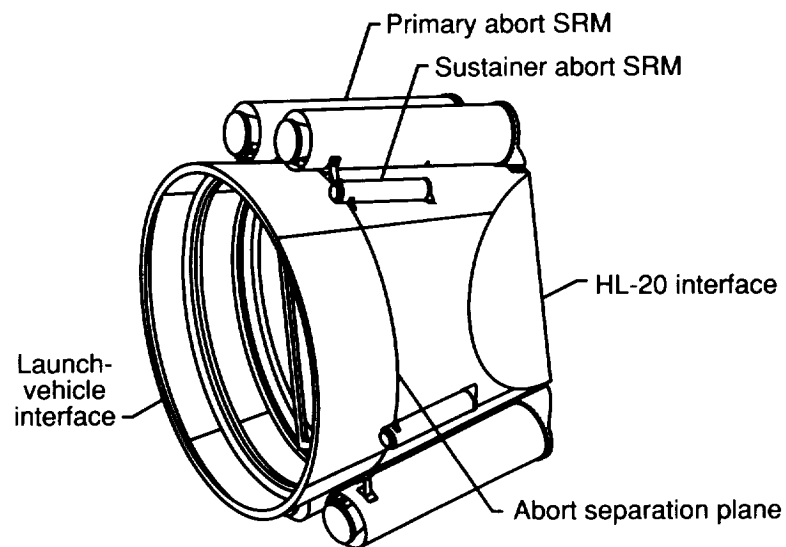
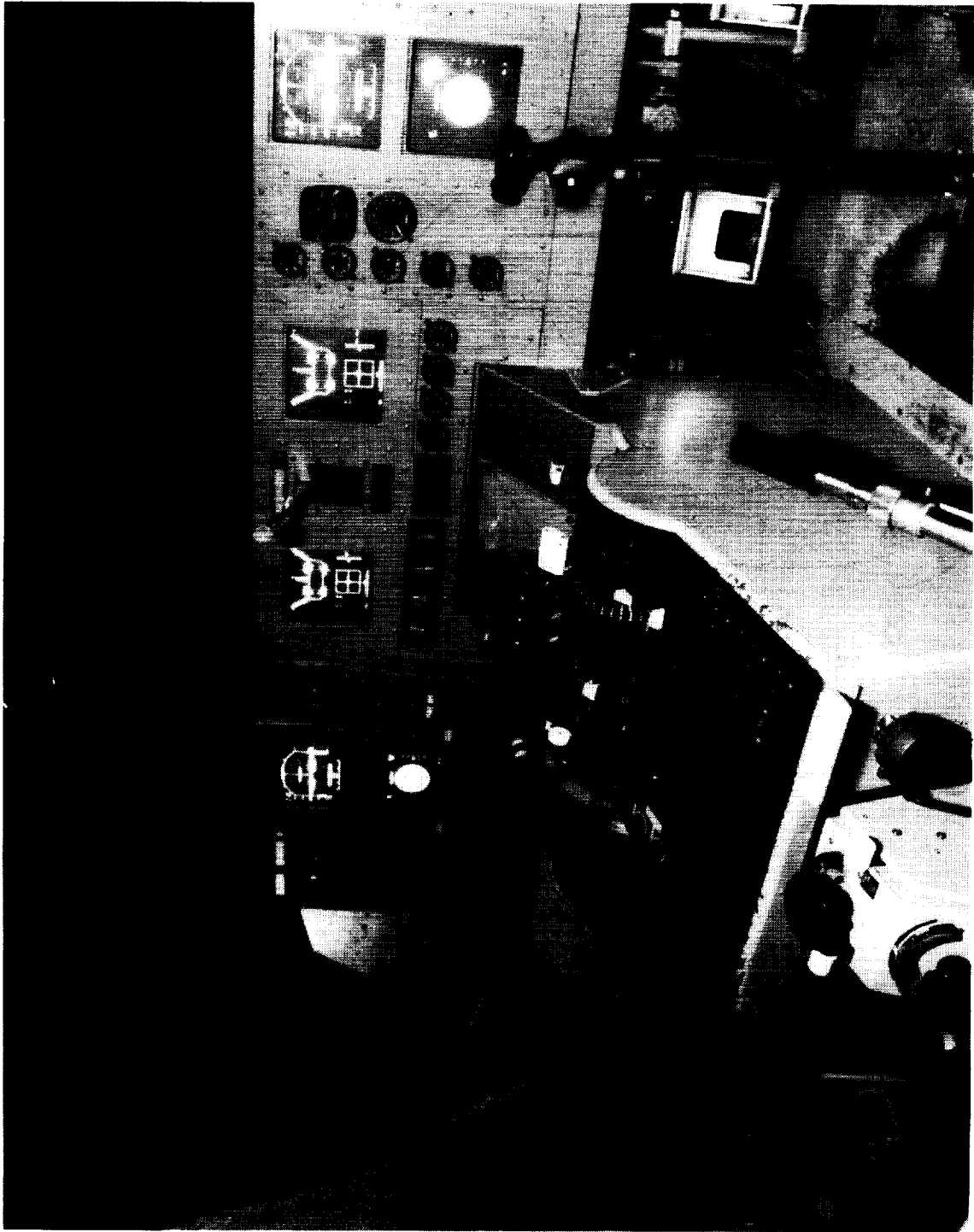


Figure 2. HL-20 launch escape system adapter with abort motors.



L-91-4568

Figure 3. Left seat of simulation cockpit.

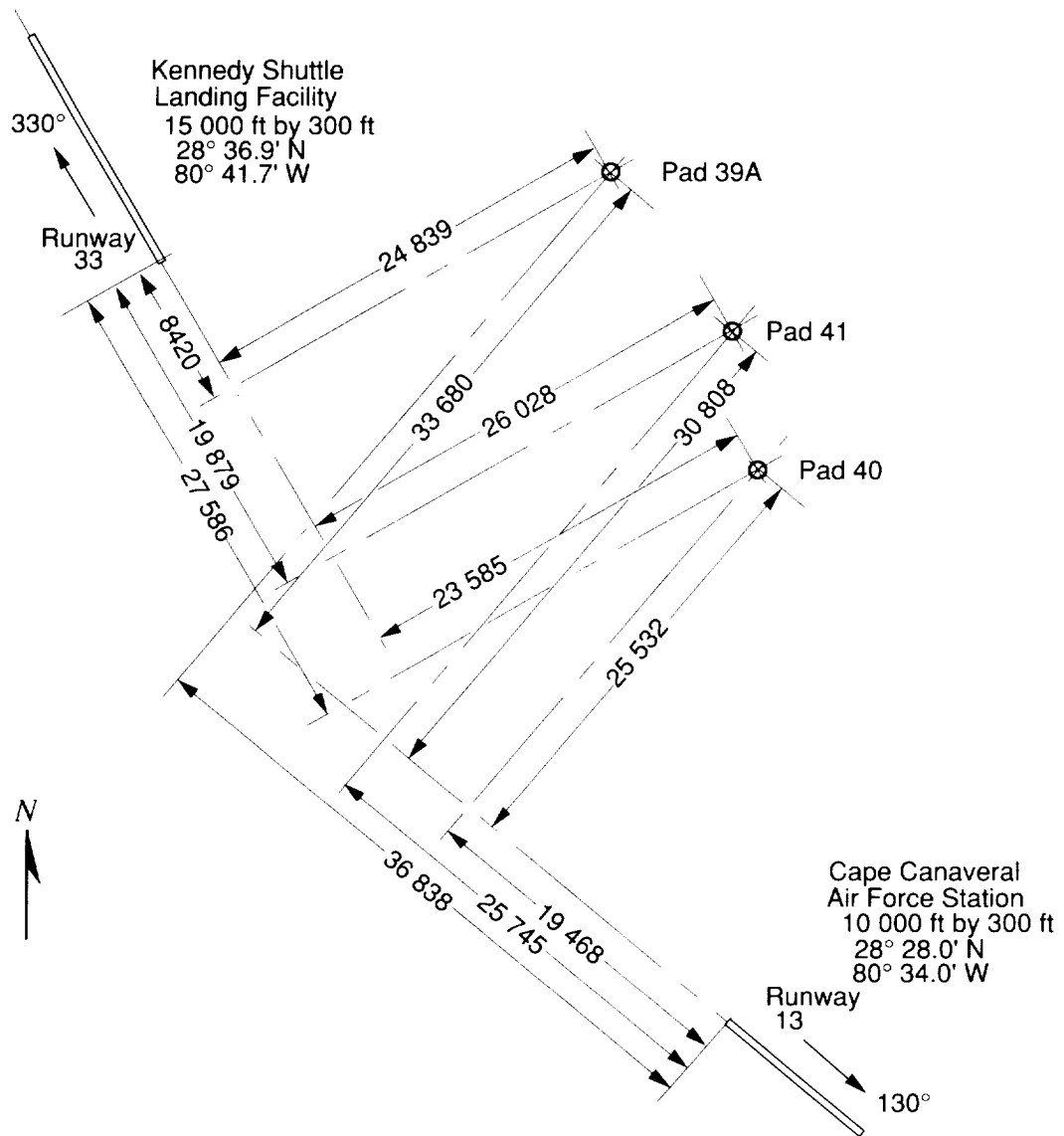


Figure 4. Possible launch pad-abort-to-runway geometries. Linear dimensions are in feet.

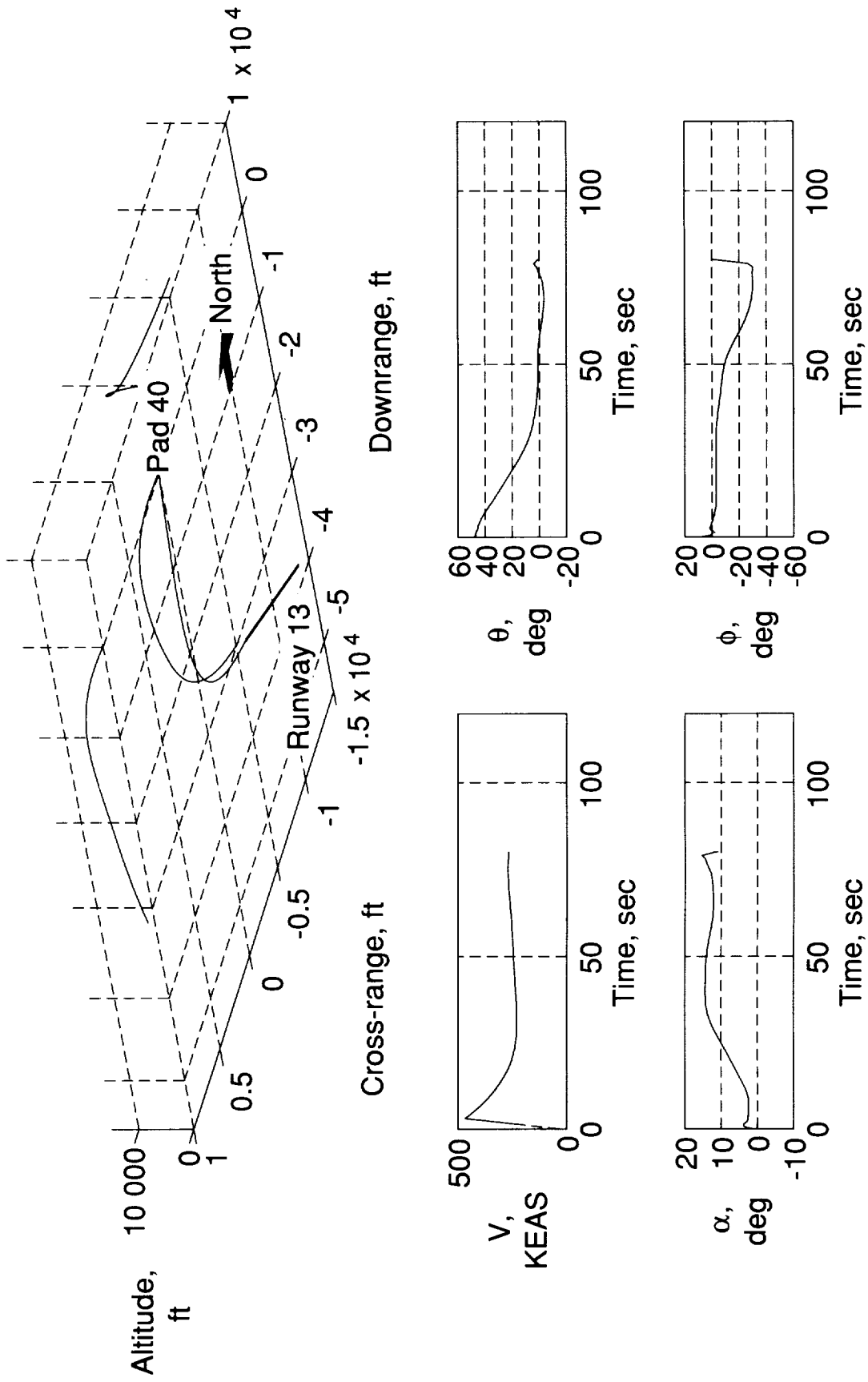


Figure 5. Optimal trajectory for pad 40 to runway-13 abort.

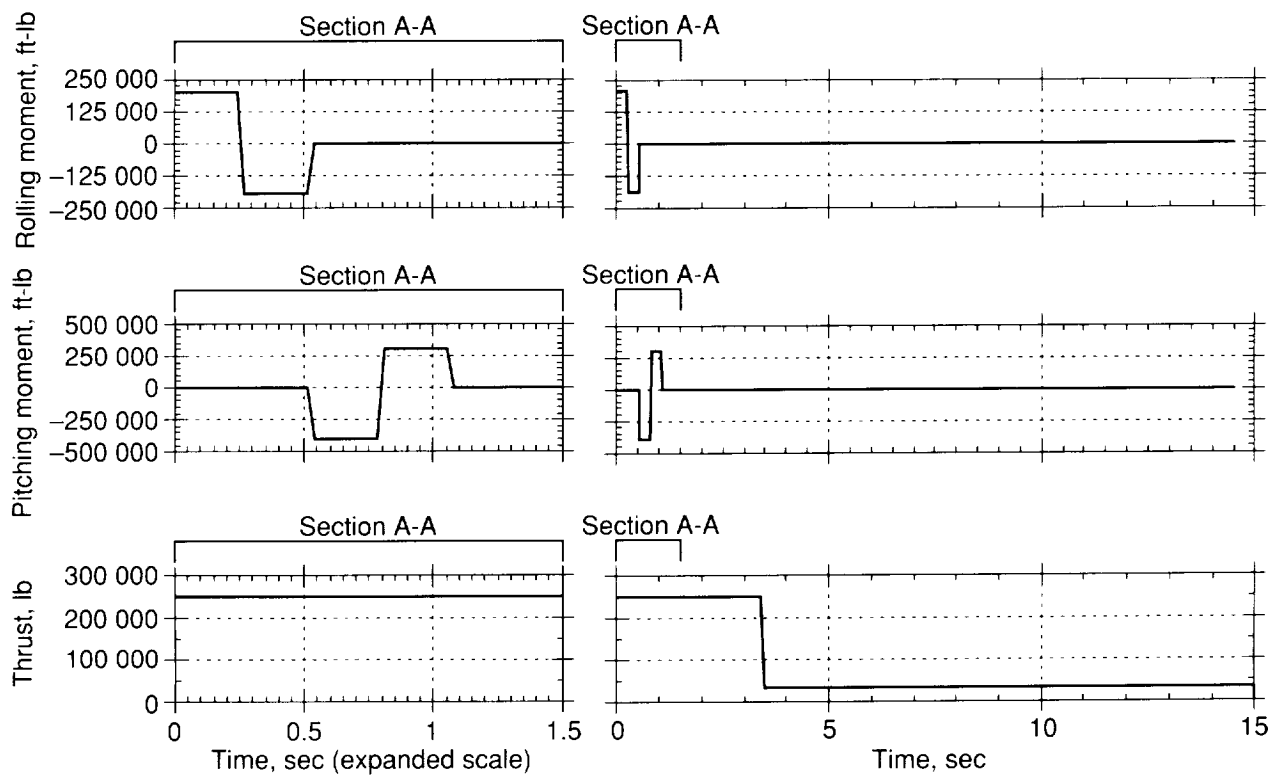


Figure 6. Abort-motor thrust and moment profiles for pad 39A to runway-13 abort.

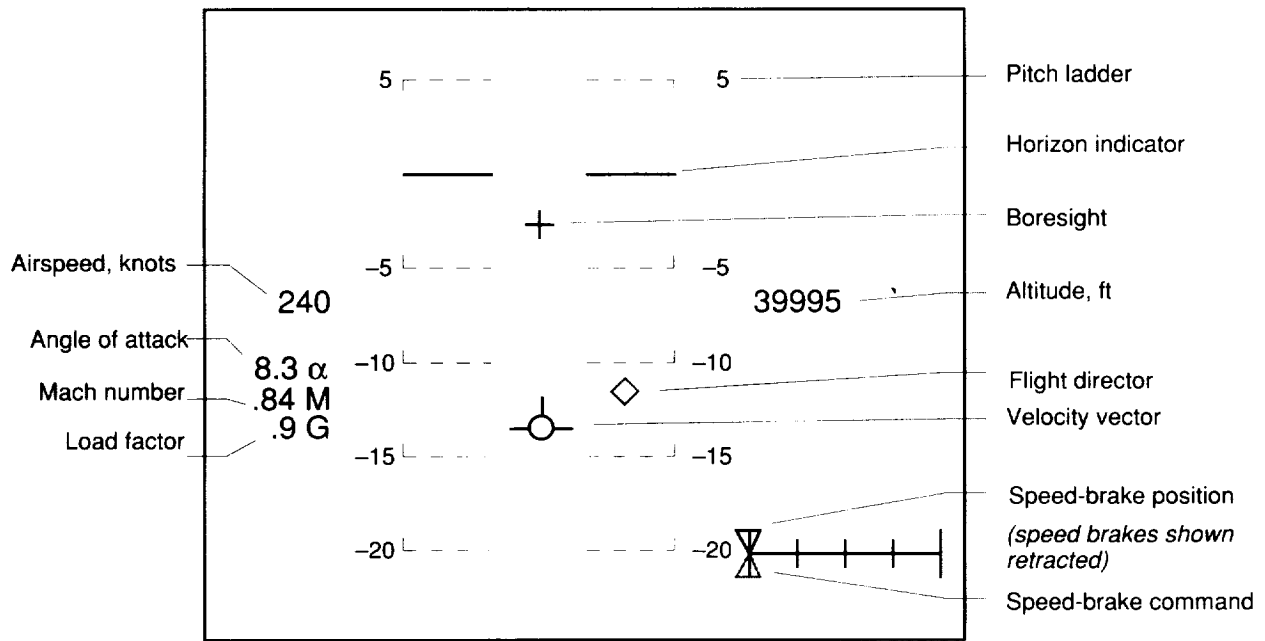


Figure 7. Schematic of head-up display.

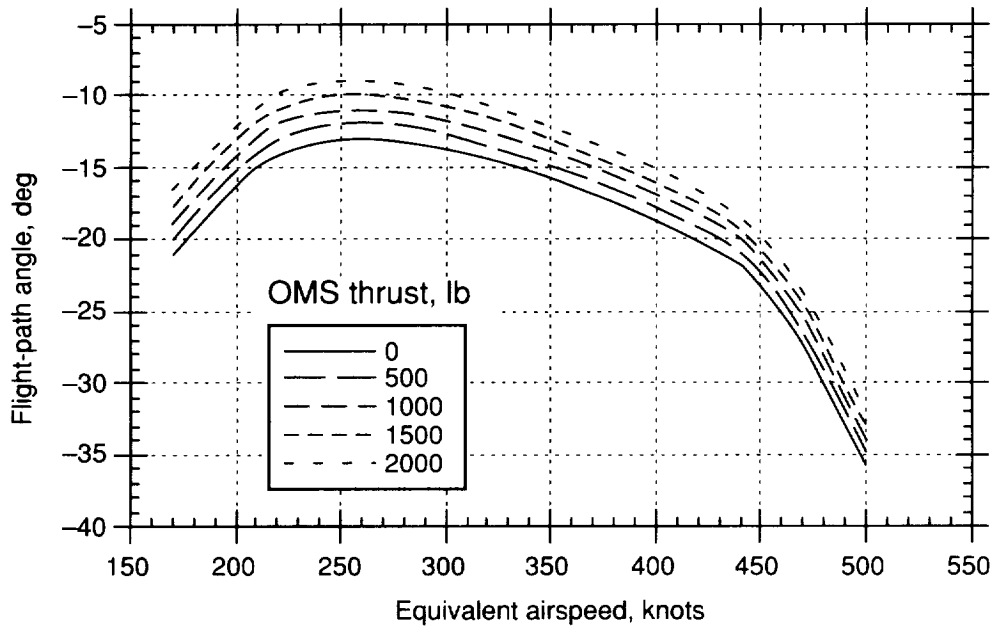


Figure 8. Steady glide trim conditions for abort configuration at altitude of 10 000 ft.

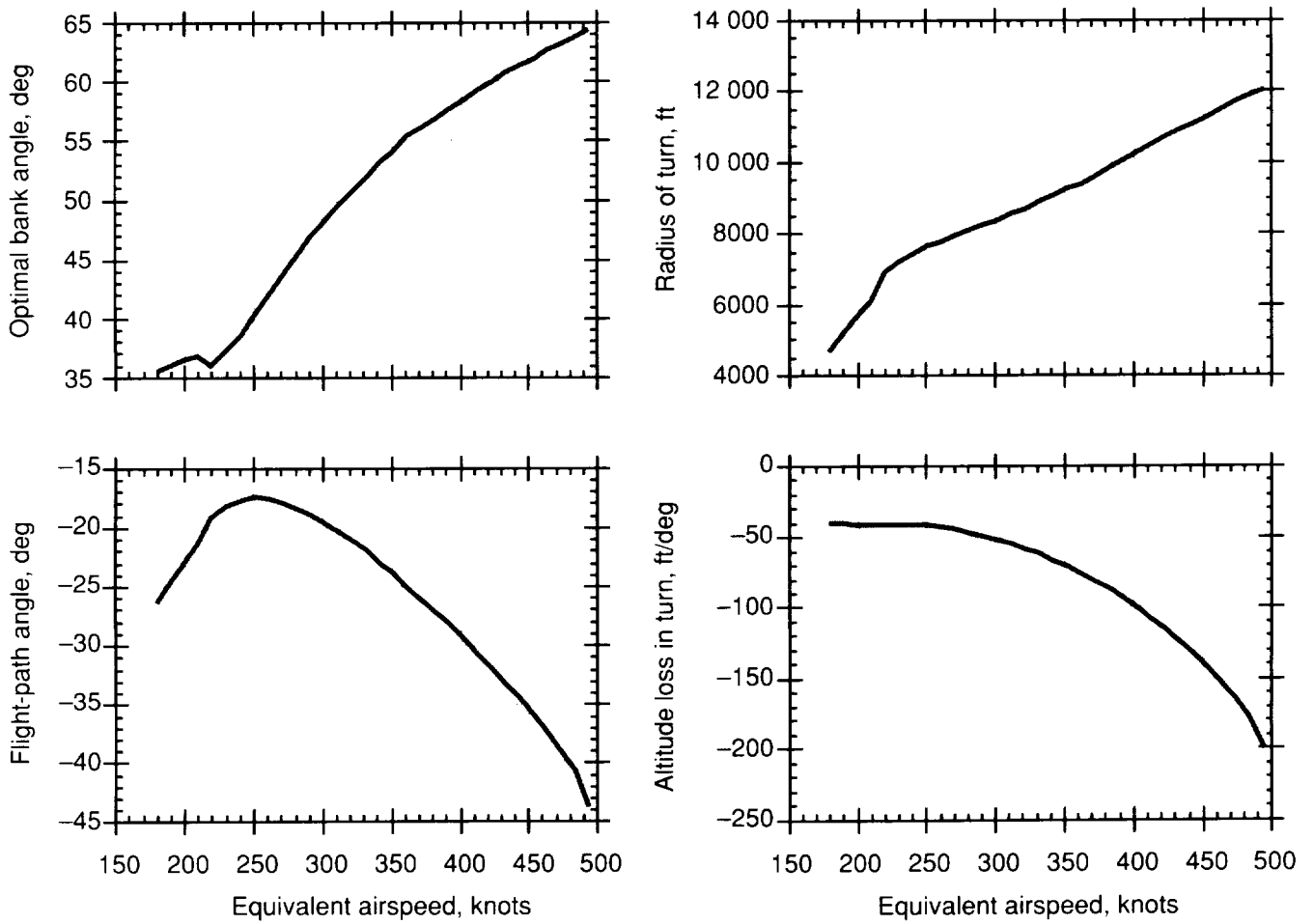


Figure 9. Most efficient steady turn performance versus airspeed.

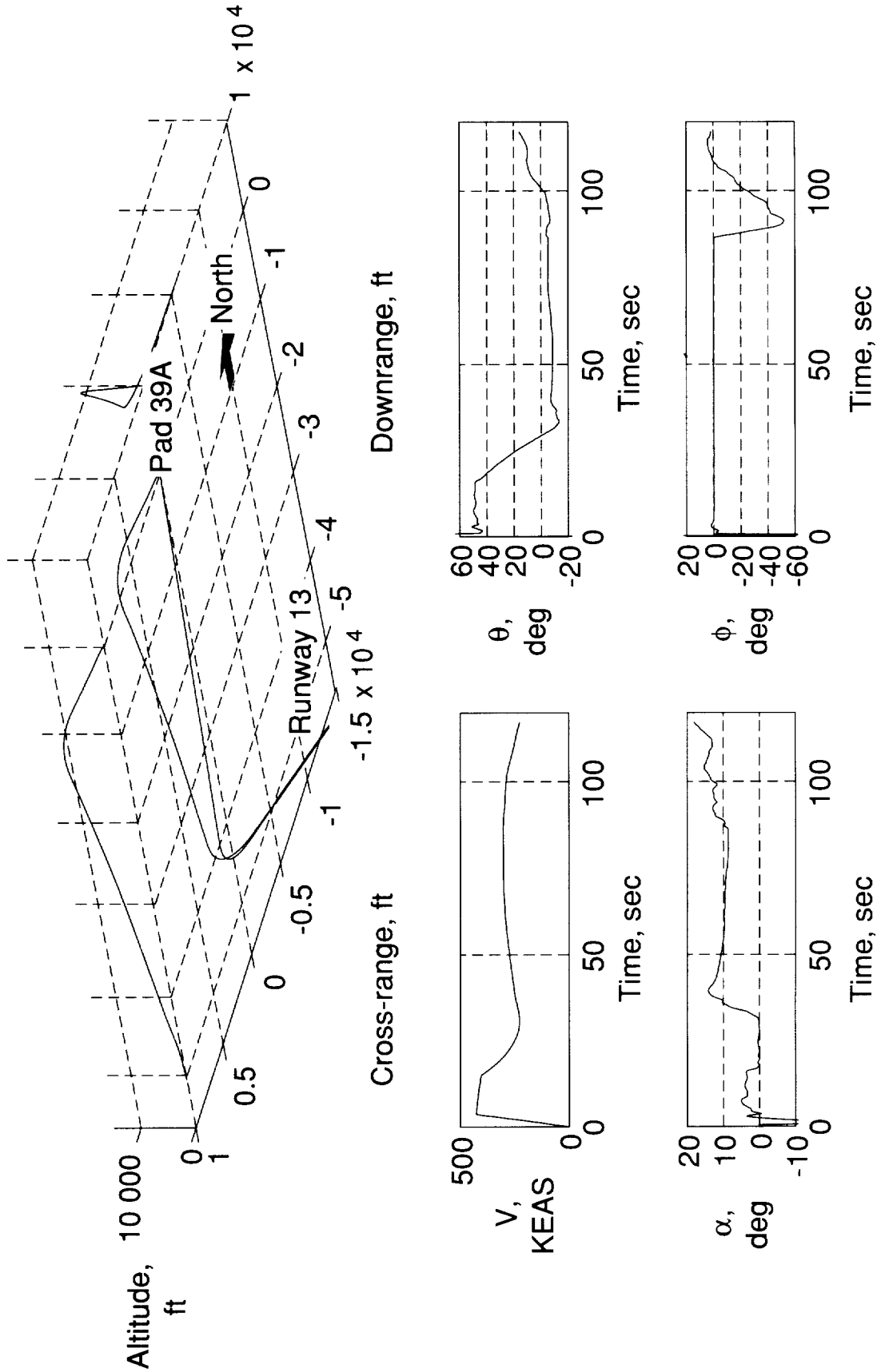


Figure 10. Heuristically derived manual abort trajectory.

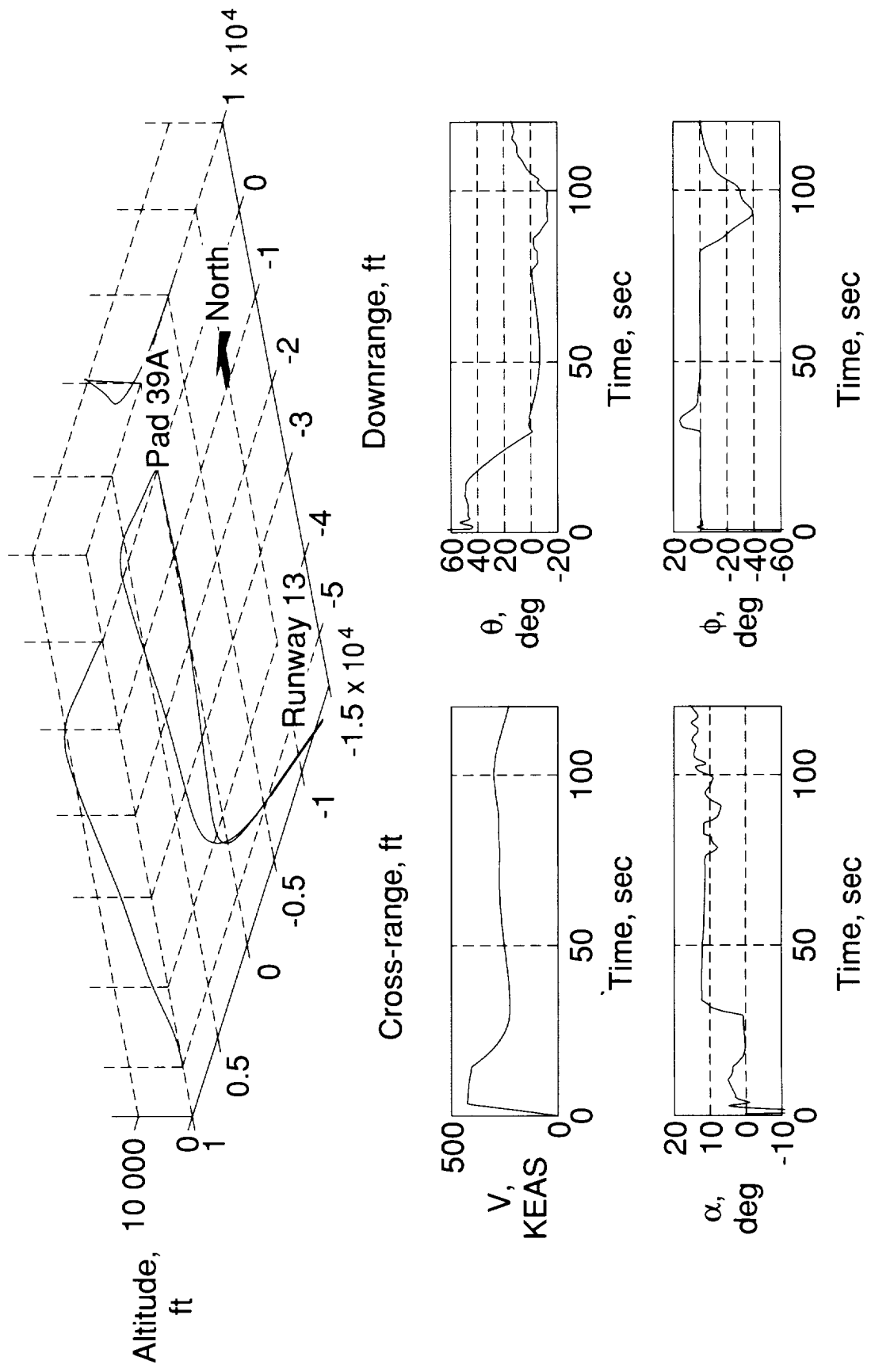


Figure 11. Heuristic abort trajectory flown by autoland system.

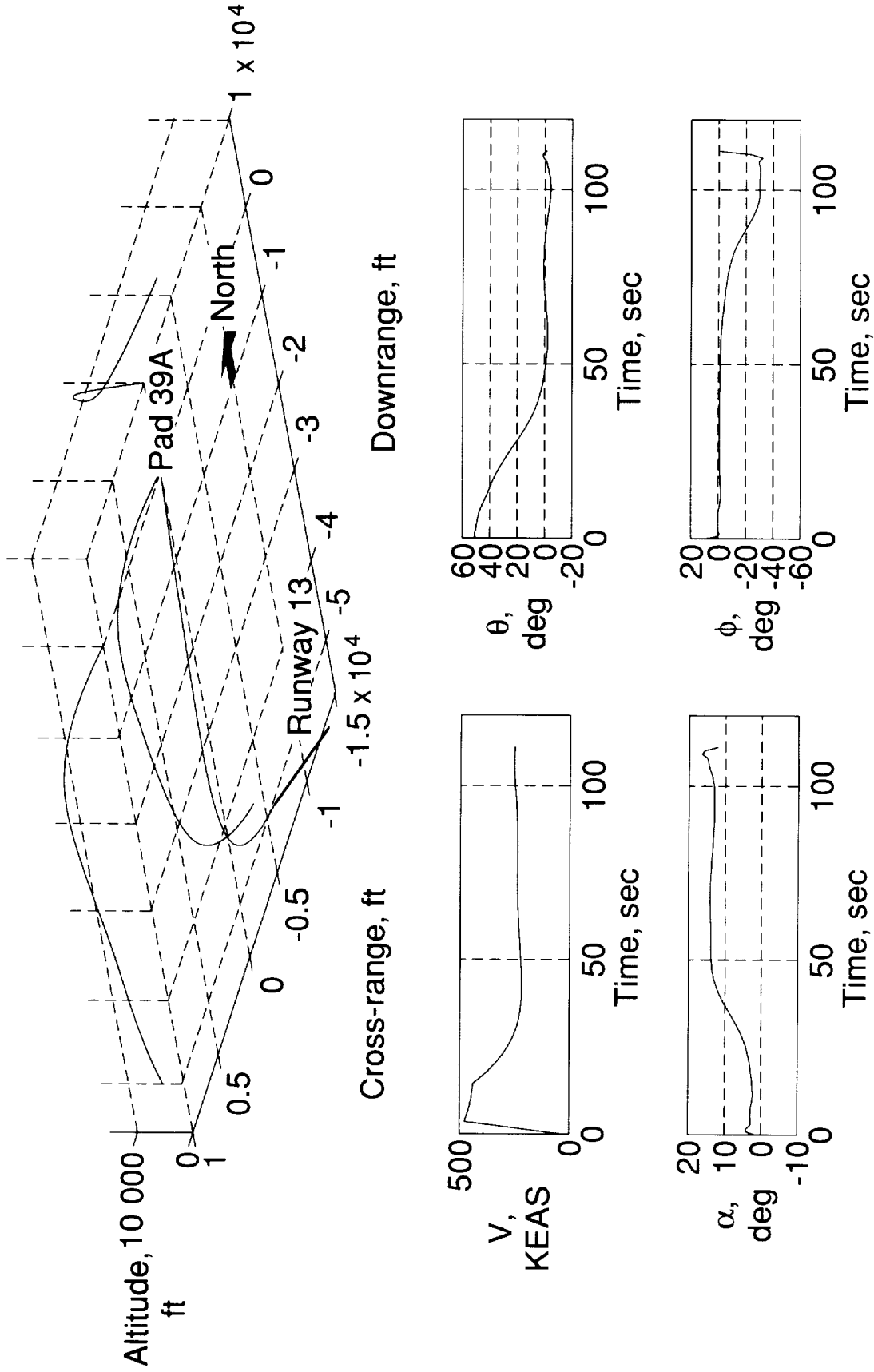


Figure 12. Optimal trajectory for pad 39A to runway-13 abort.

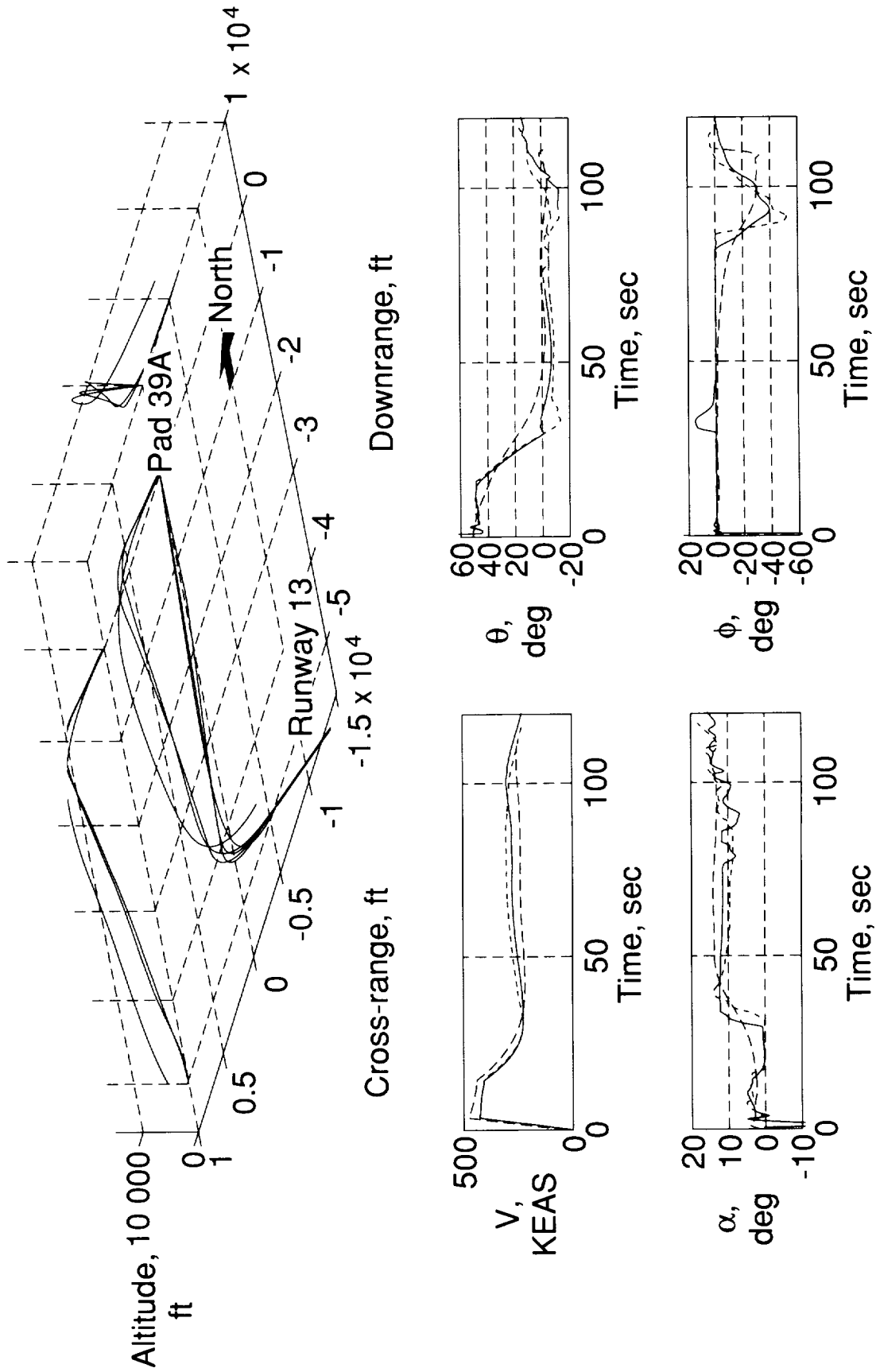


Figure 13. Comparison plot of manual, automatic, and optimal abort trajectories.

REPORT DOCUMENTATION PAGE			Form Approved OMB No. 0704-0188	
Public reporting burden for this collection of information is estimated to average 1 hour per response, including the time for reviewing instructions, searching existing data sources, gathering and maintaining the data needed, and completing and reviewing the collection of information. Send comments regarding this burden estimate or any other aspect of this collection of information, including suggestions for reducing this burden, to Washington Headquarters Services, Directorate for Information Operations and Reports, 1215 Jefferson Davis Highway, Suite 1204, Arlington, VA 22202-4302, and to the Office of Management and Budget, Paperwork Reduction Project (0704-0188), Washington, DC 20503				
1. AGENCY USE ONLY(Leave blank)	2. REPORT DATE May 1994	3. REPORT TYPE AND DATES COVERED Technical Memorandum		
4. TITLE AND SUBTITLE Launch-Pad Abort Capabilities of the HL-20 Lifting Body			5. FUNDING NUMBERS WU 505-64-52-01	
6. AUTHOR(S) E. Bruce Jackson, Robert A. Rivers, Rajiv S. Chowdhry, W. A. Ragsdale, and David W. Geyer				
7. PERFORMING ORGANIZATION NAME(S) AND ADDRESS(ES) NASA Langley Research Center Hampton, VA 23681-0001			8. PERFORMING ORGANIZATION REPORT NUMBER L-17330	
9. SPONSORING/MONITOPING AGENCY NAME(S) AND ADDRESS(ES) National Aeronautics and Space Administration Washington, DC 20546-0001			10. SPONSORING/MONITORING AGENCY REPORT NUMBER NASA TM-4550	
11. SUPPLEMENTARY NOTES E. Bruce Jackson and Robert A. Rivers: Langley Research Center, Hampton, Virginia; Rajiv S. Chowdhry: Lockheed Engineering & Sciences Company, Hampton, Virginia; W. A. Ragsdale and David W. Geyer: Unisys Corporation, Hampton, Virginia.				
12a. DISTRIBUTION/AVAILABILITY STATEMENT Unclassified Unlimited Subject Category 08			12b. DISTRIBUTION CODE	
13. ABSTRACT (Maximum 200 words) The capability of the HL-20 lifting body to perform an abort maneuver from the launch pad to a horizontal landing was studied. The study involved both piloted and batch simulation models of the vehicle. A point-mass model of the vehicle was used for trajectory optimization studies. The piloted simulation was performed in the Langley Visual/Motion Simulator in the fixed-base mode. A candidate maneuver was developed and refined for the worst-case launch-pad-to-landing-site geometry with an iterative procedure of off-line maneuver analysis followed by piloted evaluations and heuristic improvements to the candidate maneuver. The resulting maneuver demonstrates the launch-site abort capability of the HL-20 and dictates requirements for nominal abort-motor performance. The sensitivity of the maneuver to variations in several design parameters was documented.				
14. SUBJECT TERMS Lifting body; Abort; HL-20; Parametric variations; Piloted simulation; Optimal trajectory			15. NUMBER OF PAGES 18	
			16. PRICE CODE A03	
17. SECURITY CLASSIFICATION OF REPORT Unclassified	18. SECURITY CLASSIFICATION OF THIS PAGE Unclassified	19. SECURITY CLASSIFICATION OF ABSTRACT Unclassified	20. LIMITATION OF ABSTRACT	